This paper appears in IEEE Transactions on Industrial Electronics.
http://dx.doi.org/10.1109/TIE.2016.2619320

Kinematic Bilateral Tele-driving of Wheeled Mobile Robots Coupled with Slippage

Weihua Li, Liang Ding, *Member*, *IEEE*, Zhen Liu, Weidong Wang, Haibo Gao and Mahdi Tavakoli, *Member, IEEE*

***Abstract*—With the increasing applications of wheeled mobile robots (WMR) in various fields, some new challenges have arisen on designing its teleoperation system. One of such challenges is caused by wheel's slippage. This paper proposes a new approach for haptic tele-driving of a WMR coupled with slippage. In this teleoperation system, the WMR's linear velocity and angular velocity respectively follow the master haptic interface's positions. The proposed teleoperation controller also includes an acceleration-level control law for the WMR so that the WMR's linear and angular velocity loss induced by the slippage can be compensated for. Information caused by wheel's slippage in the environment termination (ET) is displayed to the human operator through haptic (force) feedback. After designing a local controller to compensate for the ET's nonpassivity caused by the slippage, the system's stability is shown via its passivity and it is also shown that the force felt by the human operator is approximately equal to the output force of the ET. Experiments of the proposed controller demonstrate that the modified ET is passive and the controller can result in stable bilateral teleoperation with a satisfactory tracking performance.**

***Index Terms*—Slippage, Telerobotics and Teleoperation, Wheeled Mobile Robots.**

I. Introduction

WHEN a wheeled mobile robot (WMR) is traveling on a slippery surface (e.g., soft sand), the ideal assumption of pure rolling [1-2], which is most considered by researchers, is not held any more, which will introduce new issues for its control. With the increasing interest in planetary (e.g., lunar) or other soft-terrain explorations by WMR, researchers have started to pay more attention to the wheel's slippage phenomenon, which induces the wheel's velocity loss compared with a desired input velocity signal [3-5]. With the introduction of slippage, the WMR's kinematic and dynamic models are affected [5], creating new challenges for its control. To compensate for the influence of the wheel's slippage on WMR's velocity, a few controllers for path-planning and tracking have been proposed in [4-5].

Tele-driving of a WMR is a natural requirement while using it in outer exploration, where appropriately providing haptic feedback can enhance the task performance [6]. For most bilateral teleoperation systems of a WMR, two kinematics-related issues exist, which are not often experienced while tele-driving of non-mobile robots [7]: 1) the workspace of the master robot is limited but that of the slave WMR is often not or much bigger, and 2) the WMR is under non-holonomic constraints as the directions of permissible motions are constrained (recently, WMRs with new configurations have been developed that can move in any directions but they are not in the scope of this paper). Owing to WMR's unlimited workspace, the coordination between master's position and slave's velocity is commonly considered [7-11]. Additionally, in order to tele-drive the WMR in the Cartesian coordinates with the non-holonomic constraints, a semi-autonomous control strategy is proposed in [11] by employing idempotent and generalized pseudo-inverse matrices to augment operator control with some level of assistance/autonomy. Generally, these researches are based on the ideal assumption of pure rolling (zero slippage). However, in applications of field WMR on loose soil, disaster exploration and scientific expedition always require tele-driving the WMR, where slippage will create new challenges. In this paper, we will consider the problem of *workspace mismatch* and *surface slippage* at the same time for a two-wheeled actuated mobile robot with the non-holonomic constraints.

Therefore, while there exists work on WMR teleoperation, the wheel's slippage is rarely considered. Typically, the WMR's embedded controller is at the kinematic level and for wheel angular velocity control (the controller ensures tracking a desired angular velocity for the wheel) rather than at the dynamic level and for wheel torque control. Using the kinematic controller for a WMR with the wheel's slippage will inevitably result in errors between the desired and actual linear/angular velocities for the WMR. To compensate for the

Manuscript received Feb 25, 2016; revised Jun 16, 2016 and Aug 11, 2016; accepted Sep 11, 2016. This work was supported by the National Natural Science Foundation of China (51275106/61370033), Foundation for Innovative Research Groups of the National Natural Science Foundation of China (51521003), the '973 project (2013CB035502), the China Scholarship Council (CSC) under grant [2013]3009, the Natural Sciences and Engineering Research Council (NSERC) of Canada under grant RGPIN 372042-09, and the Canada Foundation for Innovation (CFI) under grant LOF 28241. (All correspondence should be addressed to Liang Ding, Zhen Liu and Mahdi Tavakoli)

W. Li, L. Ding, Z. Liu, W. Wang and H. Gao are with the State Key Laboratory of Robotics and System, Harbin Institute of Technology, Harbin, China. (phone: 0086 451 8640 2037; fax: 0086 451 8641 3857; e-mails: {liweihua.08301, liuzhen_hit}@163.com, {liangding, wangweidong, gaohaibo}@hit.edu.cn)

M. Tavakoli is with the Department of Electrical and Computer Engineering, University of Alberta, Edmonton, Alberta, Canada (phone: 001 780 492 8935; e-mail: mahdi.tavakoli@ualberta.ca).

WMR's linear/angular velocity error caused by the slippage, an acceleration-level controller for the wheel is utilized, which will be described later.

In the context of teleoperation of a WMR coupled with slippage, the linear/angular velocity loss induced by the wheel's slippage can be modeled as the *environment termination (ET)* for the slave (WMR) robot. Interestingly, as we will see later, slippage fluctuations may cause this ET to exhibit a non-passive behavior, complicating the teleoperation control of the WMR. In our previous research [12-13], we have proposed some methods to address the WMR's bilateral teleoperation issues with longitudinal slippage (WMR's rotation is not considered). However, while the WMR's rotation is considered simultaneously under the non-holonomic constraint, the WMR's kinematic model will be coupled with the wheel's slippage. Therefore, this paper proposes a new method for haptic teleoperation control of a WMR coupled with wheel's slippage.

Compared with [7], this paper proposes a new teleoperation scheme that can address the wheel's slippage using a kinematic controller, while [7] presents a teleoperation system based on the ideal assumption of pure rolling using a dynamic controller. Evidently, [7] will not be satisfactory under slippage because it is not designed to account for it in terms of ensuring stability.

The rest of this paper is organized as follows: In Sec. II, the WMR's kinematic model coupled with the wheel's slippage is presented. In Sec. III, the extent of ET's non-passivity induced by the wheel's slippage is found, and in order to implement a position-velocity coordination, the master robot is modified with a local controller. In Sec. IV, a stabilizing controller for WMR bilateral teleoperation is designed while a controller is designed to compensate for the shortage of passivity (SOP) at the ET. In Sec. V, experiments of the proposed controller are done to demonstrate the system's stability and transparency. Sec. VI presents the concluding remarks and future work.

II. WMR'S KINEMATIC MODEL COUPLED WITH SLIPPAGE

In this paper, a two-wheeled differential mobile robot is researched as Fig. 1 shows. The two back wheels are driving wheels and the front wheel is free. Thus, the WMR can travel and rotate under non-holonomic constraints. In Fig. 1, it is assumed that the wheel's actual linear velocities are v_1 (left) and v_2 (right), the wheel's angular velocities are ω_1 (left) and ω_2 (right). It is assumed that the wheel's desired linear velocities are v_{1d} (left) and v_{2d} (right); in the presence of slippage, these will be different from v_1 and v_2. It is also assumed that the WMR's linear velocity is v and its angular velocity is ω while the center point P of the WMR has coordinates (x_P, y_P, θ_P); the wheel's radius is r and the WMR's width is $2b$.

For such a WMR, the following non-holonomic constraint and kinematic equation hold [2]:

$$\dot{x}_P \sin\theta_P - \dot{y}_P \cos\theta_P = 0, \tag{1}$$

$$\begin{bmatrix} v \\ \omega \end{bmatrix} = \begin{bmatrix} \cos\theta_P & \sin\theta_P & 0 \\ 0 & 0 & 1 \end{bmatrix} \begin{bmatrix} \dot{x}_P \\ \dot{y}_P \\ \dot{\theta}_P \end{bmatrix}. \tag{2}$$

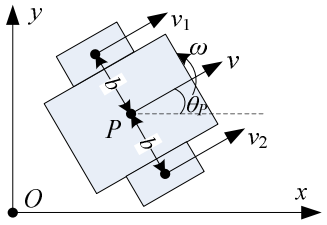

Fig.1. Kinematic scheme of a WMR.

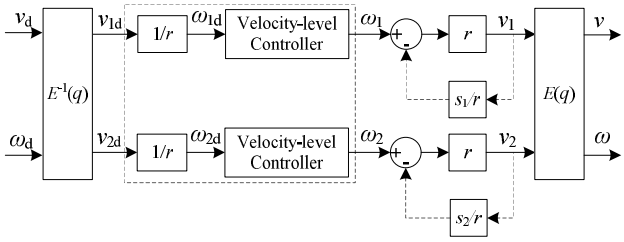

Fig. 2. WMR velocity-based control scheme.

In the ideal case of pure rolling for the WMR's wheels (no slippage), the WMR is always controlled at an angular velocity level as Fig. 2 shows. It is mostly assumed that, in Fig. 2, the transfer function from ω_{1d} (or ω_{2d}) to ω_1 (or ω_2) is ideally unity. Therefore, the WMR's kinematic model incorporating each wheel's angular velocity controller can be expressed as

$$\begin{bmatrix} v \\ \omega \end{bmatrix} = E(q) \begin{bmatrix} v_1 \\ v_2 \end{bmatrix} = E(q) \begin{bmatrix} r\omega_1 \\ r\omega_2 \end{bmatrix} = \begin{bmatrix} v_d \\ \omega_d \end{bmatrix}, \tag{3}$$

where v_d and ω_d are the controller inputs;

$$E(q) = \begin{bmatrix} \frac{1}{2} & \frac{1}{2} \\ -\frac{1}{2b} & \frac{1}{2b} \end{bmatrix}.$$

However, when the WMR is traveling on a soft terrain (e.g., loose soil), due to the limited drawbar pull force generated by the terrain and the possible opposing external forces such as those coming from hitting an obstacle, each wheel's linear velocity will not simply be equal to the wheel's angular velocity times the wheel's radius. Slippage s_1 for left wheel and slippage s_2 for right wheel can be respectively defined as [5]

$$\begin{cases} s_1 = \dfrac{r\omega_1 - v_1}{v_1} \\ s_2 = \dfrac{r\omega_2 - v_2}{v_2} \end{cases}, \tag{4}$$

As (4) shows, the slippage causes a loss of the wheel's linear velocity. However, only with the slippage, this WMR still cannot violate the non-holonomic constraint (1), implying that the WMR's lateral velocity is still zero. Thus, for the WMR's linear velocity and angular velocity in the presence of slippage, the following equation still holds:

$$\begin{bmatrix} v \\ \omega \end{bmatrix} = E(q) \begin{bmatrix} v_1 \\ v_2 \end{bmatrix}. \tag{5}$$

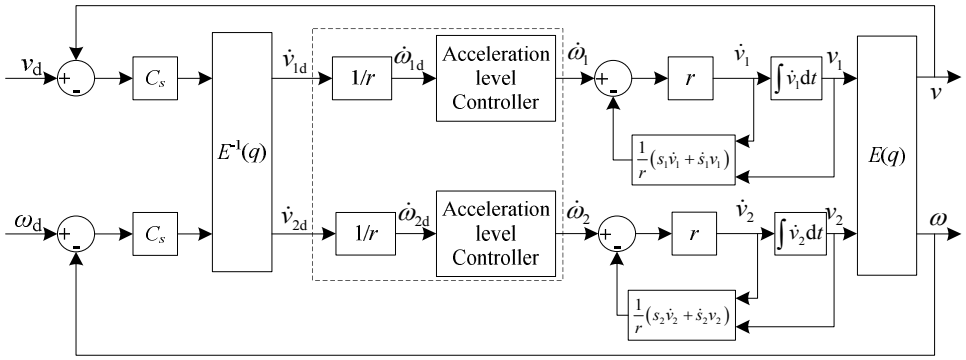

Fig. 3. WMR acceleration-based control scheme coupled with slippage.

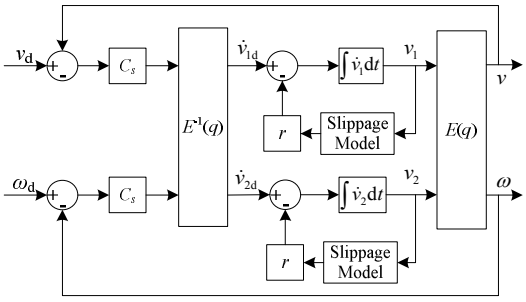

Fig. 4. Simplification of WMR acceleration-based control scheme.

Therefore, in the case of slippage, the WMR's velocity-level controller will be modified by a velocity feedback as the dashed line shown in Fig. 2.

Under the assumption that the transfer function of the WMR's velocity-level controller is unity (e.g., $\omega_{1d} = \omega_1$), we can obtain $r\omega_1 = v_{1d}$ (the same holds for the right wheel as well). Then, let's define the slippage-induced loss on the wheel's actual linear velocity compared to its desired value as

$$\begin{cases} \delta_1 = v_{1d} - v_1 \\ \delta_2 = v_{2d} - v_2 \end{cases}. \tag{6}$$

Substituting (6) into (5), we can obtain the influence of the wheel's slippage on the WMR's linear velocity and rotation velocity as

$$\begin{bmatrix} v \\ \omega \end{bmatrix} = \begin{bmatrix} v_d \\ \omega_d \end{bmatrix} - E(q) \begin{bmatrix} \delta_1 \\ \delta_2 \end{bmatrix}. \tag{7}$$

From (7), we can see that under the influence of the wheel's slippage, the tracking performance of the WMR's linear velocity and angular velocity will degrade compared to that in the pure-rolling case, if the WMR's velocity-level controller is used. Therefore, in order to have a good velocity-tracking performance in the presence of slippage, it is necessary to use an acceleration-level controller based on the difference between the WMR's actual linear velocity/angular velocity and the desired linear velocity/angular velocity as Fig. 3 shows. Similarly, the transfer function from $\dot{\omega}_{1d}$ (or $\dot{\omega}_{2d}$) to $\dot{\omega}_1$ (or $\dot{\omega}_2$) can also be assumed to be unity here. Thus, Fig. 3 can be simplified as Fig. 4. Through deriving $\begin{cases} s_1 v_1 = r\omega_1 - v_1 \\ s_2 v_2 = r\omega_2 - v_2 \end{cases}$ obtained from (4), we can get:

$$\begin{cases} r\left(\dot{\omega}_1 - \underbrace{\frac{1}{r}\left(s_1\dot{v}_1 + \dot{s}_1 v_1\right)}_{\text{Slippage Model}}\right) = \dot{v}_1 \\ r\left(\dot{\omega}_2 - \overbrace{\frac{1}{r}\left(s_2\dot{v}_2 + \dot{s}_2 v_2\right)}^{\text{Slippage Model}}\right) = \dot{v}_2 \end{cases}. \tag{8}$$

Here, it is noted that the wheel's slippage s_1 and s_2 are both time-varying functions.

Under the coupling of the WMR's translation (linear motion) and rotation, the WMR's kinematics at the acceleration-level can be modeled as

$$\begin{bmatrix} \dot{v} \\ \dot{\omega} \end{bmatrix} = E(q) \begin{bmatrix} \dot{v}_1 \\ \dot{v}_2 \end{bmatrix} + \dot{E}(q) \begin{bmatrix} v_1 \\ v_2 \end{bmatrix} = E(q) \begin{bmatrix} \dot{v}_1 \\ \dot{v}_2 \end{bmatrix}. \tag{9}$$

Substituting (8) into (9), we can obtain:

$$\begin{bmatrix} \dot{v} \\ \dot{\omega} \end{bmatrix} = E(q) \begin{bmatrix} \dot{v}_{1d} - \left(\dot{s}_1 v_1 + s_1 \dot{v}_1\right) \\ \dot{v}_{2d} - \left(\dot{s}_2 v_2 + s_2 \dot{v}_2\right) \end{bmatrix} = \begin{bmatrix} \dot{v}_d \\ \dot{\omega}_d \end{bmatrix} - \delta_e, \tag{10}$$

where, we define the loss of the WMR's linear acceleration and angular acceleration caused by wheel's slippage as δ_e where

$$\delta_e = M_{e1} \begin{bmatrix} \dot{v} \\ \dot{\omega} \end{bmatrix} + M_{e2} \begin{bmatrix} v \\ \omega \end{bmatrix}, \tag{11}$$

where,

$$M_{e1} = \begin{bmatrix} \frac{1}{2}(s_1 + s_2) & \frac{b}{2}(s_2 - s_1) \\ \frac{1}{2b}(s_2 - s_1) & \frac{1}{2}(s_1 + s_2) \end{bmatrix};$$

$$M_{e2} = \begin{bmatrix} \frac{1}{2}(\dot{s}_1 + \dot{s}_2) & \frac{b}{2}(\dot{s}_2 - \dot{s}_1) \\ \frac{1}{2b}(\dot{s}_2 - \dot{s}_1) & \frac{1}{2}(\dot{s}_1 + \dot{s}_2) \end{bmatrix}.$$

III. MASTER/SLAVE ROBOT MODEL IN A WMR'S TELEOPERATION SYSTEM

A. Slave robot model

In this section, we will consider the model (10) of a WMR coupled with slippage, which acts as the slave robot of a teleoperation system. We are interested in modeling the terrain-dependent slippage as the "environment" with which the slave robot of a teleoperation system interacts. Defining the control input $u_s = [\dot{v}_{sd} \quad \dot{\omega}_{sd}]^T$ and the environment interaction force as δ_e, the kinematic model of the slave robot can be found based on (10) and (11) as

$$\begin{bmatrix} \dot{v}_s \\ \dot{\omega}_s \end{bmatrix} = u_s - \delta_e, \tag{12}$$

where v_s and ω_s are the slave WMR's linear velocity and angular velocity.

From the definition of the slippage in (4), it looks to be only related with the wheel's linear velocity and its angular velocity. However, the slippage actually is not decided by the WMR's states, but by the wheel/terrain interaction characteristics. Therefore, δ_e in (12) can be seen as the contribution of the external environment (terrain) to deciding the WMR's linear acceleration and angular acceleration while the WMR is travelling on a slippery surface.

In this paper, we consider the case of $r\omega_1 > v_1$ and $r\omega_2 > v_2$, that is $s_1, s_2 > 0$ corresponding to the case where the wheel slippage causes a *reduction* in the linear velocity of each wheel of the WMR compared to the pure rolling case. We here assume that the change rate of slippage is constrained by $\dot{s}_{1L} < \dot{s}_1 < \dot{s}_{1U}$ and $\dot{s}_{2L} < \dot{s}_2 < \dot{s}_{2U}$, where $\dot{s}_{1L}$, $\dot{s}_{2L}$, $\dot{s}_{1U}$ and $\dot{s}_{2U}$ are decided by the WMR's states and the contacting terrain's properties.

Equation (12) provides a straightforward and useful model of the WMR as the slave robot of a teleoperation system in interaction with a slippage-dependent environment. The following properties are proposed to determine the passivity or non-passivity of the environment involved in (12).

Property 1 Matrix M_{e1} in (11) is a positive-definite matrix, if $s_1, s_2 > 0$.

Proof: For this matrix M_{e1}, its leading principle minors meet the following inequalities:

(1) 1st-order principal minor: $\frac{1}{2}(s_1 + s_2) > 0$, since $s_1, s_2 > 0$;

(2) 2nd-order principal minor: $\frac{1}{4}\left[(s_1 + s_2)^2 - (s_2 - s_1)^2\right] > 0$, since $|s_1 + s_2| > |s_2 - s_1|$.

Therefore, the matrix M_{e1} is positive-definite [17]. *End.*

Property 2 The environment system (11), when $\dot{s}_1$ and/or $\dot{s}_2$ is negative, is potentially non-passive.

Proof: With the input $[v_s \ \omega_s]$ and the output $\delta_e(t)$, the environment system (11) satisfies the following inequality for all $T \geq 0$:

$$\begin{aligned} &\int_0^T [v_s(t) \quad \omega_s(t)]\delta_e(t)dt \\ &= \underbrace{k_{se}(T) - k_{se}(0)}_{Z_{e1}} + \underbrace{\frac{1}{2}\int_0^T [v_s(t) \quad \omega_s(t)]\left(M_{e2}\begin{bmatrix} v_s \\ \omega_s \end{bmatrix}\right)dt}_{Z_{e2}} \\ &\geq -k_{se}(0) + \frac{1}{2}\int_0^T [v_s(t) \quad \omega_s(t)]\left(M_{e2}\begin{bmatrix} v_s \\ \omega_s \end{bmatrix}\right)dt, \end{aligned} \tag{13}$$

where $k_{se}(t) = \frac{1}{2}[v_s(t) \quad \omega_s(t)]M_{e1}\begin{bmatrix} v_s(t) \\ \omega_s(t) \end{bmatrix} \geq 0$, since the matrix M_{e1} is positive-definite (**Property 1**).

However, the matrix M_{e2} in (11) is potentially negative definite (as shown later) if $\dot{s}_1$ and/or $\dot{s}_2$ is negative, meaning that the component Z_{e2} in (13) is potentially non-passive [14]. Therefore, when $\dot{s}_1$ and/or $\dot{s}_2$ is negative, owing to the potentially negative definite Z_{e2}, the environment termination (11) is potentially non-passive (active), which can potentially destabilize the WMR bilateral teleoperation system. *End.*

B. Master robot model

In order to tele-drive the WMR's linear velocity and angular velocity respectively, a two-DOF (degree of freedom) robot is used as the master robot in this paper. Its dynamic model can be written as

$$M_m\ddot{X}_m + C_m\dot{X}_m = \tau_m + \tau_h, \tag{14}$$

where M_m (2×2) and C_m (2×2) are the robot's mass matrix and Coriolis/centrifugal matrix, X_m (2×1) is the joint position vector, τ_m (2×1) and τ_h (2×1) are the forces/torques applied by the robot actuators and the operator at the robot joints.

The master robot's dynamic model (14) has the following properties [15]:

(1) M_m is a positive-definite matrix;

(2) $\dot{M}_m - 2C_m$ is a skew-symmetric matrix.

Theoretically, the master robot (14) meets the following inequality for $\forall T \geq 0$,

$$\begin{aligned} &\int_0^T \dot{X}_m(\tau_m + \tau_h)dt = \int_0^T \dot{X}_m\left(M_m\ddot{X}_m + C_m\dot{X}_m\right)dt \\ &= k_{dm}(T) - k_{dm}(0) \geq -k_{dm}(0), \end{aligned} \tag{15}$$

where, $k_{dm}(t) = \frac{1}{2}\dot{X}_m M_m \dot{X}_m \geq 0$, since M_m is a positive definite matrix. Therefore, the master robot system is passive while a velocity-velocity (master-slave) mapping is used.

In general non-mobile robot teleoperation applications, the velocities (and positions) of the master and slave robots are synchronized. However, owing to the unlimited workspace of the WMR, in this paper, the master robot's DOFs and the slave robot's DOFs are mapped as the following: the WMR's linear velocity should follow the master robot's 1st joint position (1st DOF) so that (X_{m1}, v_s) track one another, and the WMR's angular velocity should follow the master robot's 2nd joint position (2nd DOF) so that (X_{m2}, ω_s) track one another.

However, when the above position-velocity mapping is considered, we can find that the energy generated by the master robot system,

$$\int_0^T X_m(\tau_m+\tau_h)dt=\int_0^T X_m\left(M_m\ddot{X}_m+C_m\dot{X}_m\right)dt\ ,$$

is no longer passive (this is unlike (15)). Inspired by [7], a new variable $r_m=\lambda\dot{X}_m+X_m$ where $0<\lambda<1$ is employed to be used instead of $\dot{X}_m$ in the impedance matrix; in this way, the problem will become one of coordinating r_m (which is a 2×1 vector) and $[v_s,\ \omega_s]^T$. When λ and/or $\dot{X}_m$ are small enough, an approximate coordination of position-velocity ($X_m\approx[v_s,\ \omega_s]^T$) is achieved between the master robot and the slave WMR.

The above change of variable also necessitates defining a new control signal. Therefore, the controller τ_m in (14) is designed as $\tau_m=\tau_m^*+\overline{\tau}_m$ consisting of a local controller τ_m^* and $\overline{\tau}_m$ that will be designed in Sec. IV. In terms of the new variable r_m and with the local controller $\tau_m^*=-B_{mv}\dot{X}_m-B_{mp}X_m$, the master robot's dynamic model (14) can be rewritten as

$$M_m\ddot{X}_m+\left(C_m+B_{mv}\right)\dot{X}_m+B_{mp}X_m=\overline{\tau}_m+\tau_h. \tag{16}$$

Then, through designing the local controller τ_m^*, by the following property, the modified master system (16) can be guaranteed to be passive with the new variable $r_m=\lambda\dot{X}_m+X_m$.

Property 3 Given a coefficient λ for r_m, when $B_{mv}=M_m/\lambda$ and $B_{mp}=C_m/\lambda$, the dynamic system (16) with the local controller (τ_m^*) meets the following passivity criterion: for all r_m and $T\ge 0$,

$$\int_0^T r_m\left(\overline{\tau}_m+\tau_h\right)dt\ge k_m(T)-k_m(0)\ge -k_m(0)\ ,$$

where, $k_m(t)$ is a positive-definite function.

Proof: Based on the master robot's dynamic model (16), we can obtain the system's energy with the new variable r_m as

$$\begin{aligned}&\int_0^T r_m\left(\overline{\tau}_m+\tau_h\right)dt=\int_0^T r_m\left(M_m\ddot{X}_m+\left(C_m+B_{mv}\right)\dot{X}_m+B_{mp}X_m\right)dt\\&=\int_0^T\left(r_m\frac{M_m}{\lambda}\left(\lambda\ddot{X}_m+\dot{X}_m\right)+r_m\frac{C_m}{\lambda}\left(\lambda\dot{X}_m+X_m\right)\right)dt+\\&\int_0^T\left(r_m\left(B_{mv}-\frac{M_m}{\lambda}\right)\dot{X}_m+r_m\left(B_{mp}-\frac{C_m}{\lambda}\right)X_m\right)dt\ ,\\&=\underbrace{k_{d1}(T)-k_{d1}(0)}_{Z_{m1}}+\underbrace{\int_0^T r_m\left(B_{mv}-\frac{M_m}{\lambda}\right)\dot{X}_m dt}_{Z_{m2}}+\underbrace{\int_0^T r_m\left(B_{mp}-\frac{C_m}{\lambda}\right)X_m dt}_{Z_{m3}}\end{aligned}$$

where $k_{d1}(t)=\frac{1}{2}\left(\lambda\dot{X}_m+X_m\right)^T\frac{M_m}{\lambda}\left(\lambda\dot{X}_m+X_m\right)\ge 0$, since M_m is a positive-definite matrix.

Therefore, to guarantee the master robot's passivity, the local controller parameter B_{mv} and B_{mp} should be designed to make $B_{mv}=M_m/\lambda$ and $B_{mp}=C_m/\lambda$. In this case, we can obtain

$$\int_0^T r_m\left(\overline{\tau}_m+\tau_h\right)dt\ge -k_{d1}(0)=-k_m(0). \tag{17}$$

In conclusion, for a given coefficient λ of the dynamic parameter r_m, if the local controller parameters B_{mv} and B_{mp} meet that $B_{mv}=M_m/\lambda$ and $B_{mp}=C_m/\lambda$, the augmented master robot is passive with the new variable r_m. Specially, if two one-DOF robots are combined to work as the master robot, which are common in the tele-driving of WMR (one maps the WMR's translation, and the other maps the WMR's rotation), since C_m is 0 in this case, B_{mp} is not necessary any more. *End.*

In addition, the human operator model should also be written in terms of the new variable r_m. However, as [7] and our previous research [12] presented, we assume the human operator can adjust his/her impedance to ensure the passivity of his/her impedance when augmented with the position/velocity transformation. This assumption is often seen in an overwhelming majority of the teleoperation literature [16].

IV. Design of WMR Bilateral Teleoperation System

According to the above analysis, the WMR's bilateral teleoperation system can be designed as Fig. 5 shows. In Fig. 5, MCU encompasses the master and its controller. SCU consists of the slave and its controller. HT is the human termination, ET is the environment termination, and CC is the communication channel. In this system, the communication time delay is not considered. Time delay can be dealt with using many approaches – see [15] for a survey. We are focusing on the special problems in the WMR bilateral teleoperation system caused by the WMR and the wheel's slippage in this paper.

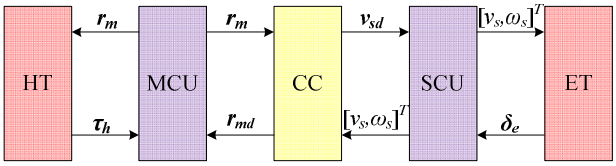

Fig. 5. Scheme of WMR's bilateral teleoperation.

In the proposed teleoperation system, the slippage-dependent interaction is dynamically generated between the WMR and the environment (terrain); here, this interaction is modeled by an equivalent force. The proposed force feedback is meant to provide feedback about slippage to the human operator so that the human operator can better drive the mobile robot in unknown environments.

A. Compensation for ET's non-passivity

As (13) shows, the ET is potentially non-passive to some extent, and becomes a destabilizing factor in the WMR bilateral teleoperation system. Therefore, in this section, we will first design an additional controller in order to compensate for the ET's non-passivity. Based on (13), we can obtain the potential non-passive component of the ET as Z_{e2}.

For the matrix M_{e2} in Z_{e2}, it has different properties while the values of $\dot{s}_{1L}$ and $\dot{s}_{2L}$ are changing.

Similar with **Property 1**, when both $\dot{s}_{1L}$ and $\dot{s}_{2L}$ are positive, the ET is strictly passive. However, when $\dot{s}_{1L}$ and/or $\dot{s}_{2L}$ is negative, the matrix M_{e2} is potentially negative-definite, in which case Z_{e2} becomes a potentially non-passive component. Therefore, based on the proposed non-passivity compensation methods in our previous research [12], the following local

controller is proposed to compensate for the ET's non-passivity as Fig. 6 shows:

$$\bar{u}_{SOP}=\begin{bmatrix} -\frac{1}{4}\left(\dot{s}_{1L}+\dot{s}_{2L}\right) & -\frac{b}{4}\left(\dot{s}_{2L}-\dot{s}_{1L}\right) \\ -\frac{1}{4b}\left(\dot{s}_{2L}-\dot{s}_{1L}\right) & -\frac{1}{4}\left(\dot{s}_{1L}+\dot{s}_{2L}\right) \end{bmatrix}\begin{bmatrix} v_s \\ \omega_s \end{bmatrix}=\varepsilon_e\begin{bmatrix} v_s \\ \omega_s \end{bmatrix}, \quad (18)$$

where ε_e is the compensation matrix and can be designed by the following process.

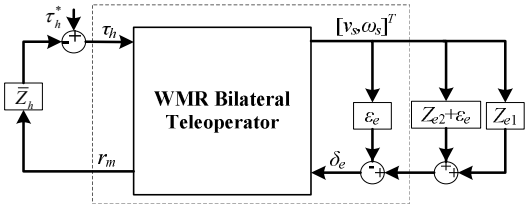

Fig. 6. Compensation for the ET's non-passivity.

After applying (18) to compensate for the ET's non-passivity, the potential non-passive component Z_{e2} is modified as

$$\bar{Z}_{e2}=\frac{1}{2}\int_0^T\begin{bmatrix} v_s(t) \\ \omega_s(t) \end{bmatrix}^T\left(\bar{M}_{e2}\begin{bmatrix} v_s \\ \omega_s \end{bmatrix}\right)dt, \quad (19)$$

where, $\bar{M}_{e2}=M_{e2}+\varepsilon_e$.

Property 4 The matrix $\bar{M}_{e2}$ in (19) is positive semi-definite, when $\dot{s}_{1L}$ and $\dot{s}_{2L}$ are negative.

Proof: For the matrix $\bar{M}_{e2}$, its leading principle minor meets the following inequalities:

(1) 1st-order principal minor:

$$\frac{1}{2}\left(\dot{s}_1-\dot{s}_{1L}+\dot{s}_2-\dot{s}_{2L}\right)\geq 0,$$

since $\dot{s}_1-\dot{s}_{1L}\geq 0$ and $\dot{s}_2-\dot{s}_{2L}\geq 0$;

(2) 2nd-order principal minor:

$$\frac{1}{4}\left(\dot{s}_1-\dot{s}_{1L}+\dot{s}_2-\dot{s}_{2L}\right)^2-\frac{1}{4}\left(\dot{s}_2-\dot{s}_{2L}-\dot{s}_1+\dot{s}_{1L}\right)^2\geq 0,$$

since $\left|\dot{s}_1-\dot{s}_{1L}+\dot{s}_2-\dot{s}_{2L}\right|\geq\left|\dot{s}_2-\dot{s}_{2L}-\dot{s}_1+\dot{s}_{1L}\right|$.

Therefore, the matrix $\bar{M}_{e2}$ is positive semi-definite. *End.*

As a result, with (18), $\bar{Z}_{e2}$ is positive semi-definite for any input $[v_s,\ \omega_s]^T$, and this component in the ET is passive. Therefore, the whole modified ET is passive, combining **Property 2** and **Property 4**.

In general cases, when $\dot{s}_{1L}$ and/or $\dot{s}_{2L}$ are negative, it makes sense to assume $\dot{s}_{1L}=\dot{s}_{2L}=-\varepsilon_{SOP}$, since the WMR's left wheel and right wheel run on the same terrain with a similar states. Therefore, the compensation matrix in (18) can be written as

$$\varepsilon_e=\begin{bmatrix} \frac{1}{2}\varepsilon_{SOP} & 0 \\ 0 & \frac{1}{2}\varepsilon_{SOP} \end{bmatrix}. \quad (20)$$

With (18) to compensate for the ET's non-passivity at the slave site, the slave robot's model (12) is modified as

$$\begin{bmatrix} \dot{v}_s \\ \dot{\omega}_s \end{bmatrix}=u_s-\left(\bar{u}_{SOP}+\delta_e\right)=u_s-\bar{\delta}_e, \quad (21)$$

where $\bar{\delta}_e$ is the modified environment termination after the compensation for the ET's non-passivity, which is passive.

B. Design of WMR bilateral teleoperation system

After the compensation for the ET's non-passivity with (18), this section will design the WMR teleoperation system's controllers to guarantee its stability and transparency. As mentioned above, the coordination between the master robot and the slave robot is to happen between the pairs (r_{m1}, v_s) and also between the pairs (r_{m2}, ω_s).

Aiming at the coordination of (r_{m1}, v_s), the controllers for the master robot and the slave robot are respectively designed as

$$\begin{cases} \bar{\tau}_{m1}=-k_v\left(r_{m1}(t)-v_s(t)\right) \\ \dot{v}_{sd}=-k_v\left(v_s(t)-r_{m1}(t)\right) \end{cases} \quad (22)$$

Similarly for (r_{m2}, ω_s), the controllers are designed as

$$\begin{cases} \bar{\tau}_{m2}=-k_\omega\left(r_{m2}(t)-\omega_s(t)\right) \\ \dot{\omega}_{sd}=-k_\omega\left(\omega_s(t)-r_{m2}(t)\right) \end{cases} \quad (23)$$

In (25) and (26), k_v and k_ω are both positive.

Theorem 1 Consider the WMR bilateral teleoperation system consisting of the slave robot (21) with the local controller (18), and the master robot (16) with the local controller ($\tau_m^*=-B_{mv}\dot{X}_m-B_{mp}X_m$), which meets the modified passivity (17). Also consider the teleoperation controllers (22) and (23).

1) The closed loop teleoperator is passive, in the sense that $\exists$ a finite d s.t. $\forall T\geq 0$,

$$\int_0^T\left[\left(\tau_{h1}r_{m1}+\tau_{h2}r_{m2}\right)-\left(\bar{\delta}_{e1}v_s+\bar{\delta}_{e2}\omega_s\right)\right]dt\geq -d^2.$$

2) The human operator is assumed to be passive and the modified slippage-induced environment system (19) is proved to be passive, that is: $\exists$ finite d_1 and d_2 s.t. $\forall T\geq 0$,

$$\int_0^T\left(\tau_{h1}r_{m1}+\tau_{h2}r_{m2}\right)dt\leq d_1^2,\quad \int_0^T-\left(\bar{\delta}_1v_s+\bar{\delta}_2\omega_s\right)dt\leq d_2^2. \quad (24)$$

Then, r_{m1}, r_{m2}, v_s and ω_s are all bounded $\forall t\geq 0$; as a result, (r_{m1}-v_s) and (r_{m2}-ω_s) are also bounded $\forall t\geq 0$.

3) Suppose that

$$\left(\ddot{X}_{m1}(t),\dot{X}_{m1}(t),\ddot{X}_{m2}(t),\dot{X}_{m2}(t),\dot{v}_s(t),\dot{\omega}_s(t)\right)\to 0$$

(that is the master robot and the slave robot are stable at a certain state). Then, $\tau_{h1}\to k_v\left(X_{m1}-v(t)\right)\to-\bar{\delta}_{e1}$, which implies the human operator can perceive the interaction force between the slave robot and the environment. Similarly, for the $\left(r_{m2},\omega_s\right)$ pair, we also have $\tau_{h2}\to k_\omega\left(X_{m2}-\omega_s(t)\right)\to-\bar{\delta}_{e2}$.

Proof: 1) Based on the controllers (22) and (23) of the WMR bilateral teleoperation system, we can obtain

$$\begin{cases} \bar{\tau}_{m1}r_{m1}+u_1v_s=-k_v\left(r_{m1}-v_s\right)^2\leq 0 \\ \bar{\tau}_{m2}r_{m2}+u_2\omega_s=-k_\omega\left(r_{m2}-\omega_s\right)^2\leq 0 \end{cases} \quad (25)$$

Based on these two properties, combining the passivity analysis for the master robot (17) and the slave robot, we can obtain:

$$\begin{aligned}&\int_0^T\left[\left(\tau_{h1}r_{m1}+\tau_{h2}r_{m2}\right)-\left(\bar{\delta}_{e1}v_s+\bar{\delta}_{e2}\omega_s\right)\right]dt\\&=\int_0^T\left(\tau_{h1}r_{m1}+\tau_{h2}r_{m2}+\bar{\tau}_{m1}r_{m1}+\bar{\tau}_{m2}r_{m2}\right)dt\\&+\int_0^T\left(u_1v_s-\bar{\delta}_{e1}v_s+u_2\omega_s-\bar{\delta}_{e2}\omega_s\right)dt\\&-\int_0^T\left[\left(\bar{\tau}_{m1}r_{m1}+u_1v_s\right)+\left(\bar{\tau}_{m2}r_{m2}+u_2\omega_s\right)\right]dt\\&\geq k_m(T)-k_m(0)+k_s(T)-k_s(0)\\&\geq -k_m(0)-k_s(0)=-d^2,\end{aligned}\tag{26}$$

where $k_m(t)$ and $k_s(t)$ are the energy functions for the master robot and the slave robot, all of which are nonnegative as the above analysis shows:

$$k_m(t)=\frac{1}{2}r_m^T\frac{M_m}{\lambda}r_m\geq 0,\ k_s(t)=\frac{1}{2}\begin{bmatrix}v_s & \omega_s\end{bmatrix}\begin{bmatrix}v_s\\ \omega_s\end{bmatrix}\geq 0.$$

2) Based on (26), combining the given human operator's passivity and the given environment's passivity (24), we can obtain

$$k_m(T)-k_m(0)+k_s(T)-k_s(0)\leq d_1^2+d_2^2.\tag{27}$$

That is

$$\frac{1}{2}r_m^T\frac{M_m}{\lambda}r_m+\frac{1}{2}\begin{bmatrix}v_s & \omega_s\end{bmatrix}\begin{bmatrix}v_s\\ \omega_s\end{bmatrix}\leq d_1^2+d_2^2+k_m(0)+k_s(0).\tag{28}$$

Therefore, r_{m1}, r_{m2}, v_s and ω_s are all bounded $\forall t\geq 0$. As a result, (r_{m1}-v_s) and (r_{m2}-ω_s) are also bounded.

3) Since $\left(\ddot{X}_{m1}(t),\dot{X}_{m1}(t),\ddot{X}_{m2}(t),\dot{X}_{m2}(t),\dot{v}_s(t),\dot{\omega}_s(t)\right)\to 0$, combining their respective controllers, and in the case of $B_{mp}=C_m/\lambda$, the slave robot's model and the master robot's model are degenerated as

$$\begin{pmatrix}\tau_{h1}\\ \tau_{h2}\\ \bar{\delta}_{e1}\\ \bar{\delta}_{e2}\end{pmatrix}\to\begin{pmatrix}k_v\left(X_{m1}-v_s(t)\right)\\ k_\omega\left(X_{m2}-\omega_s(t)\right)\\ k_v\left(v_s(t)-X_{m1}\right)\\ k_\omega\left(\omega_s(t)-X_{m2}\right)\end{pmatrix}.\tag{29}$$

That is, $\tau_{h1}\to k_v\left(X_{m1}-v_s(t)\right)\to-\bar{\delta}_{e1}$ and $\tau_{h2}\to k_\omega\left(X_{m2}-\omega_s(t)\right)\to-\bar{\delta}_{e2}$, which implies the human operator can perceive the interaction force between the slave robot and the environment, and the proposed WMR bilateral teleoperation system has a good transparency. *End.*

V. Case Studies

In the case studies below, we consider the tele-driving of a WMR in an environment with soft terrain. Many literatures show that the wheel's slippage varies with the wheel/terrain contact characteristics (e.g., friction angle) [18-19] and the terrain's parameters (e.g., slope angle). Therefore, while these parameters vary with the terrain, the slippage is possible to decrease, which makes the environment be non-passive. However, limited by implementation issues concerning recreating specific terrain characteristics that give rise to certain shortage of passivity of the environment system, we perform semi-physical experiments to validate the proposed WMR bilateral teleoperation system with wheel's slippage.

A. Experimental setup

To validate the proposed methods, an experimental system is implemented using a Phantom Premium 1.5A haptic device (master robot) and ROSTDyn (slave robot).

1) Master robot and human operator

In our WMR's bilateral teleoperation system (Fig. 7), the master robot is a Phantom Premium 1.5A haptic device (Geomagic Inc., Wilmington, MA, USA), and the slave robot (WMR) is a simulation platform named ROSTDyn which was developed by the authors [19], and the communication between the master robot and the slave robot is implemented using the local area network (LAN). Considering only two degrees of freedom motion, the first joint q_1 and the second joint q_2 of the Phantom is used and the third joint is locked by a high gain position controller (q_3=0). Based on the research results from [20], the Phantom's inertia matrix is founded as M_m, and the Coriolis matrix is found as C_m. In (16), λ=0.1 and B_{mv} and B_{mp} are designed to meet $B_{mv}=M_m/\lambda$ and $B_{mp}=C_m/\lambda$.

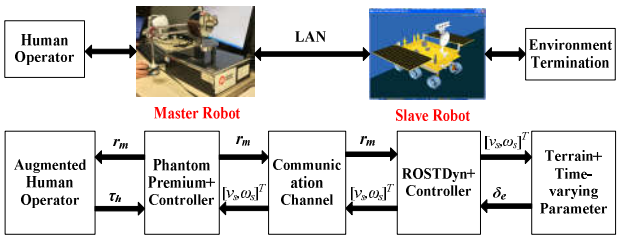

(a) Scheme of WMR bilateral teleoperation system.

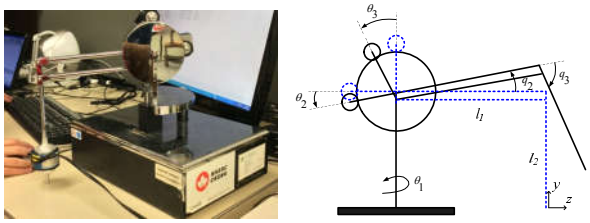

(b) The master Phantom 1.5A robot.

Fig. 7. Experimental platform of WMR bilateral teleoperation system.

In the experiments, based on (16), the torques applied on the master robot by the human operator are estimated as

$$\tau_h=M_m\ddot{X}_m+\left(C_m+B_{mv}\right)\dot{X}_m+B_{mp}X_m-\bar{\tau}_m.\tag{30}$$

2) Slave robot and environment

In the experimental system, ROSTDyn is used as the slave robot，which is developed based on Vortex software (CMLabs, Montreal, Canada) and the simplified terramechanics model especially for soft terrains (e.g., wheel's sinkage and slippage). ROSTDyn can realize a real-time simulation with good fidelity [19]. The following equation is the terramechanics model between the wheel and terrain in ROSTDyn:

$$\begin{cases}F_{\mathrm{N}}=rb\sigma_m A+rb\tau_m B=AX+BY\\ F_{\mathrm{DP}}=rb\tau_m A-rb\sigma_m B=AY-BX\\ M_{\mathrm{R}}=r^2b(\theta_1-\theta_2)\tau_m/2=rCY\end{cases},\tag{31}$$

where $A=\frac{\cos\theta_m-\cos\theta_2}{\theta_m-\theta_2}+\frac{\cos\theta_m-\cos\theta_1}{\theta_1-\theta_m}$;

$B=\frac{\sin\theta_m-\sin\theta_2}{\theta_m-\theta_2}+\frac{\sin\theta_m-\sin\theta_1}{\theta_1-\theta_m}$; $C=(\theta_1-\theta_2)/2$;

$X=rb\sigma_m$; $Y=rb\tau_m$; $\tau_m=E(c+\sigma_m\tan\varphi)$;

$\sigma_m=K_s r^N(\cos\theta_m-\cos\theta_1)^N$; $K_S=K_c/b+K_\varphi$; $N=n_0+n_1 s$;

$E=1-\exp\{-r[(\theta_1-\theta_m)-(1-s)(\sin\theta_1-\sin\theta_m)]/K\}$.

In (31), F_N is the normal force, F_{DP} is the drawbar pull force, M_R is the moment generated by the interaction between the wheel and the terrain, s is the wheel's slippage and φ is the internal friction angle. The other parameters are defined in [19]. This model mainly connects the WMR's dynamics and wheel's sinkage and slippage. For the normal force F_N, its magnitude is mostly decided by the wheel's sinkage. The softer the terrain is (corresponding to the parameter K_s), the bigger the sinkage is. Similarly, if the load in the moving direction increases, the required drawbar pull force will increase and, as a result, the wheel's slippage increases.

From [21], it is known that the wheel's slippage is influenced by many parameters. In the following experiments, the most sensitive parameter (φ) to the slippage (in practice, φ is varying since soil's properties are often different at different positions), is considered and set as a terrain-varying function.

The used terrain has a slope with an angle of 15°, and its size is 10m (x)×10m (y). The following model on the soil's internal friction angle makes the terrain become harder as the WMR travels forward, while it is same at the y axis:

$$\varphi=\begin{cases}0.55 & (0<x<3.1)\\ 0.55+0.15(x-3.1) & (3.1\le x<8.1)\\ 1.3 & (x\ge 8.1)\end{cases}. \quad (32)$$

Here, x is the WMR position along the X axis. In the case of climbing a sloped terrain, the bigger the φ is, the smaller the slippage is.

In the following experiments, the master robot provides r_m, which acts as a reference value for the slave WMR's v_s or ω_s. Owing to the time-varying slippage, the actual slave WMR's velocity v_s or ω_s may be different from its desired value and a velocity-error is caused, which is fed back to the master robot as a force. If r_m is bigger than v_s or ω_s, a backward force will be felt by the human operator that pushes back on the master robot. If r_m is smaller than v_s or ω_s, a forward force will be felt by the human operator that pulls the master robot forward. Therefore, in the proposed teleoperation system, force feedback guides the human operator to give a more effective command.

B. Experimental results

In the experiments involving WMR bilateral teleoperation coupled with the wheel's slippage, the teleoperator parameters in (22) and (23), and the compensation parameter of the ET's non-passivity in (18) are set to be:

Case I: $k_v=8; k_\omega=8; \varepsilon_e=0$;

Case II: $k_v=8; k_\omega=8; \varepsilon_e=\begin{bmatrix}0.5 & 0\\ 0 & 0.5\end{bmatrix}$.

The experimental results are shown in Fig. 8 (Case I) and Fig. 9 (Case II). In the figures, the ET's energy is calculated as $E_v=\int_o^T \bar{\delta}_{e1} v_s dt$, $E_\omega=\int_o^T \bar{\delta}_{e2}\omega_s dt$, and the whole energy generated by the actual environment system is $E=E_v+E_\omega$.

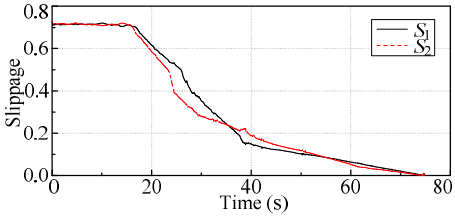

(a) Terrain/WMR slippage.

(S_1 for the left wheel, S_2 for the right wheel)

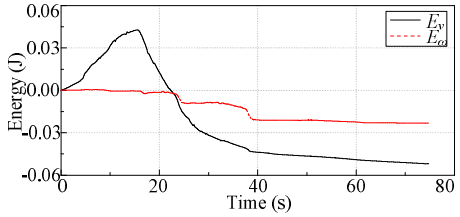

(b) Energy generated by ET.

Fig. 8. Experimental results with Case I.

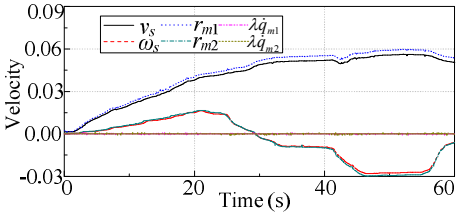

(a) Position-velocity coordination.

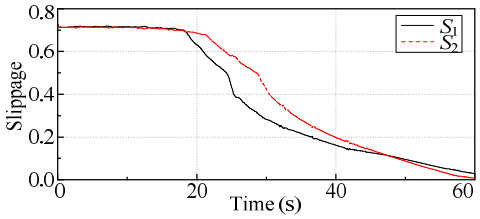

(b) Terrain/WMR slippage.

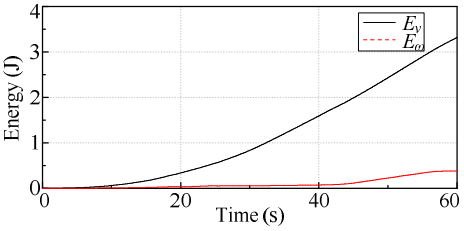

(c) Energy generated by ET.

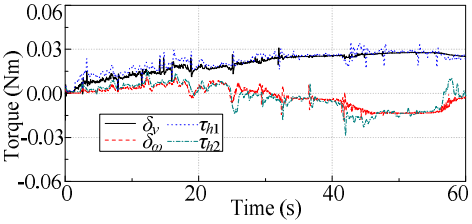

(d) Force tracking performance (τ_h and δ_e).

Fig. 9. Experimental results with Case II.

From the experimental results of Fig. 8 and Fig. 9, we can obtain the following conclusions:
1) Under the given terrain parameters (terrain-varying φ), the WMR/terrain environment is a non-passive system (Fig. 8 (b)) owing to the time-decreasing slippage (Fig. 8 (a)).
2) Since the ET (including E_v and E_ω) is non-passive, without the non-passivity compensation, the WMR bilateral teleoperation system is potentially unstable (Case I).
3) By utilizing the proposed non-passivity compensation controller (18), which is decided by the slippage curve (Fig. 9 (b)) and it makes sense that it is equal to $\varepsilon_e = \begin{bmatrix} 0.5 & 0 \\ 0 & 0.5 \end{bmatrix}$, based on the analysis in Sec. IV. The modified ET becomes strictly passive (Fig. 9 (c)) and presents a damping characteristic to some extent.
4) With the modified passive ET, the teleoperation system is stable (Fig. 9 (a)), and the human operator feels like interacting with a damping (Fig. 9 (d)), which is caused by the conservative compensation controller (18).
5) The system's force tracking performance is good. From the results, we can see that the human force is almost equal to the actual environment output force (Fig. 9 (d)), as the theory predicts in (29).

C. Experiments with a real WMR

As Fig. 10 shows, a real two-wheeled differential WMR is used as the slave mobile robot, a Novint Falcon haptic interface is used as the master robot, a motion capture system (Motive: Body, NaturalPoint Inc., Corvallis, USA) is tracking the WMR through tracking markers attached to the WMR, and the communication is done by a LAN. In the following experiments, the WMR is moving on a loose soil within a flat terrain.

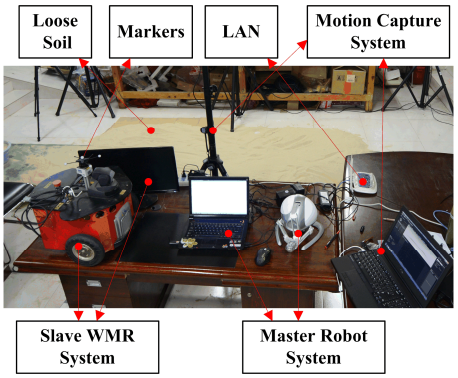

Fig. 10. Experimental system with a real WMR.

First, an experiment using a traditional velocity controller for the WMR is done (i.e., the master robot's position is directly sent to the WMR and as wheel motor's desired velocity value), which obvisouly cannot maintain a good velocity trakcing performance, as shown in Fig. 11, due to the existing slippage between the wheels and terrain. On a soft terrain, to obtain a good velocity tracking performance, the proposed teleoperation scheme in this paper can be utilized. Under the proposed teleoperation scheme, an experiment with a big slippage reduction is done, which intends to show how the big fluctuations of the slippage destabilizes the teleoperation system. In this case, the controller parameters are set as $k_v = 5; k_\omega = 5; \varepsilon_e = 0$. The results are shown in Fig. 12. In this experiment, an obstacle is used to create a big initial slippage. After 21 seconds, the obstacle is removed, so that a big reduction in slippage happens. From the results, we can see that the WMR's velocity increases quickly while the slippage is decreasing, and to some extent the operator is incapable of controlling the WMR. The operator will feel like being driven by the slave WMR.

In the third experiment, the controller parameters are set as $k_v = 5; k_\omega = 5; \varepsilon_e = \begin{bmatrix} 0.2 & 0 \\ 0 & 0.2 \end{bmatrix}$. The results are shown in Fig. 13. We can see that, the designed teleoperation system is stable, the velocity tracking performance is improved greatly, and the force transparency is also good.

By using the proposed method, the operator can estimate the WMR's states (linear velocity v_s and angular velocity ω_s) well, since the unknown velocity loss induced by the slippage (Fig. 11) is compensated for. Therefore, the operator feels like interacting with unknown environment in Fig. 11, while the operator can feel the environment termination correctly through the haptic interface with the proposed method as Fig. 13 shows.

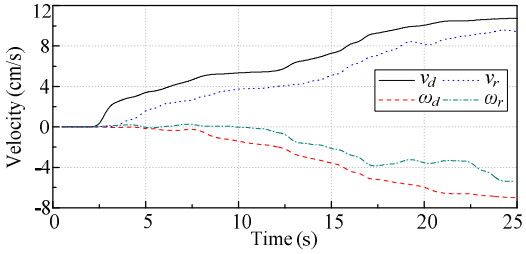

Fig. 11. Experimental results with traditional velocity controller (v_d and ω_d are the desired velocities, v_r and ω_r are the real velocities, and the haptic feedback is the difference between them).

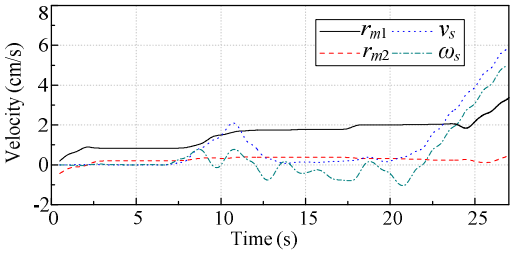

(a) Position-velocity coordination.

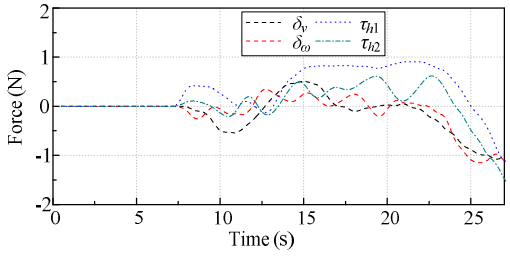

(b) Force tracking performance (τ_h and δ_e).

Fig. 12. Experimental results with a big fluctuation slippage.

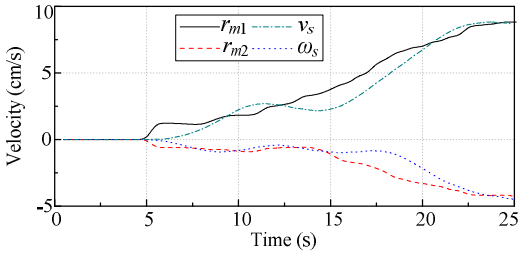

(a) Position-velocity coordination.

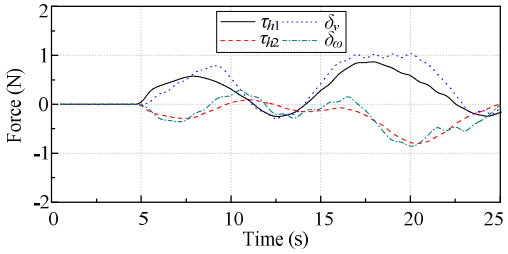

(b) Force tracking performance (τ_h and δ_e).

Fig. 13. Experimental results with proposed controller in this paper.

In conclusion, the good position-velocity tracking and force tracking performance show that the proposed WMR bilateral teleoperation system in this paper is stable and has a good transparency while the WMR is subject to the wheel's slippage.

VI. CONCLUSION

A new method for haptic tele-driving of a WMR coupled with the wheel's slippage is proposed in this paper. In this teleoperation system, the mobile robot's linear velocity and angular velocity respectively follow the master haptic interface's positions. We propose a teleoperation controller including an acceleration-level control law for the mobile robot such that the WMR's linear and angular velocity loss caused by wheel's slippage is compensated for. Another contribution of the paper lies in showing the non-passivity of the teleoperation system's environment termination coupled with the wheel's slippage. This paper then provides a stability analysis of the teleoperation system through decomposing the non-passive ET into a passive component and an active component. After designing a controller to compensate for the environment termination's non-passivity, stabilizing teleoperation controllers can then be designed via guaranteeing its passivity as shown in the paper. Experiments of the proposed controllers demonstrate the validity of the theoretical findings. In the future, the WMR's longitudinal sliding and lateral sliding can be considered in the stability analysis and control design, as well as the communication time-delay.

REFERENCES

[1] N. Uchiyama, T. Hashimoto, S. Sano and S. Takagi, "Model-Reference Control Approach to Obstacle Avoidance for a Human-Operated Mobile Robot," *IEEE Trans. Ind. Electron.*, vol. 56, no. 10, pp. 3892-3896, Oct. 2009.

[2] S. Blažic, "On Periodic Control Laws for Mobile Robots," *IEEE Trans. Ind. Electron.*, vol. 61, no. 7, pp. 3660-3670, Jul. 2014.

[3] L. Ding, K. Nagatani, K. Sato, et al., "Terramechanics-based high-fidelity dynamics simulation for wheeled mobile robot on deformable rough terrain," in *Proc. IEEE Int. Conf. Robot. Autom.*, 2010, pp. 4922–4927.

[4] G. Ishigami, K. Nagatani and K. Yoshida, "Path Following Control with Slip Compensation on Loose Soil for Exploration Rover," in *Proc. IEEE/RSJ Int. Conf. Intell. Robots Syst.*, 2006, pp. 5552-5557.

[5] Y. Tian and N. Sarkar, "Control of a Mobile Robot Subject to Wheel Slip," *J. Intell. Robot Syst.*, vol. 74, no. 4, pp. 915-929, Jun. 2014.

[6] Y. Nakajima, T. Nozaki and K. Ohnishi, "Heartbeat Synchronization With Haptic Feedback for Telesurgical Robot," *IEEE Trans. Ind. Electron.*, vol. 61, no. 7, pp. 3753-3764, Jul. 2014.

[7] D. Lee, O. M. Palafox, and M. W. Spong, "Bilateral Teleoperation of a Wheeled Mobile Robot over Delayed Communication Network," in *Proc. IEEE Int. Conf. Robot. Autom.*, 2006, pp. 3298-3303.

[8] Y. Tipsuwan and M. Y. Chow, "Gain Scheduler Middleware: A Methodology to Enable Existing Controllers for Networked Control and Teleoperation—Part II: Teleoperation," *IEEE Trans. Ind. Electron.*, vol. 51, no. 60, pp. 1228-1237, Dec. 2004.

[9] O. Linda and M. Manic, "Self-Organizing Fuzzy Haptic Teleoperation of Mobile Robot Using Sparse Sonar Data," *IEEE Trans. Ind. Electron.*, vol. 58, no. 8, pp. 3187-3195, Aug. 2011.

[10] H. V. Quang, I. Farkhatdinov and J. H. Ryu, "Passivity of Delayed Bilateral Teleoperation of Mobile Robots with Ambiguous Causalities: Time Domain Passivity Approach," in *Proc. IEEE/RSJ Int. Conf. Intell. Robots Syst.*, 2012, pp. 2635-2640.

[11] P. Malysz and S. Sirouspour, "A Task-space Weighting Matrix Approach to Semi-autonomous Teleoperation Control," in *Proc. IEEE/RSJ Int. Conf. Intell. Robots Syst.*, 2011, pp. 645-652.

[12] W. Li, L. Ding, H. Gao and M. Tavakoli, "Kinematic bilateral teleoperation of wheeled mobile robots subject to longitudinal slippage," *IET Control Theory & Applications*, vol. 10, no. 2, pp. 111-118, Jan. 2016.

[13] W. Li, L. Ding, H. Gao and M. Tavakoli, "Trilateral Predictor-mediated Teleoperation of a Wheeled Mobile Robot with Slippage," *IEEE Robotics and Automation Letters*, vol.1, no. 2, pp. 738-745, Jul. 2016.

[14] R. Lozano, B. Maschke, B. Brogliato and O. Egeland. Dissipative Systems Analysis and Control: Theory and Applications. *Springer-Verlag New York, Inc.*, Secaucus, NJ, USA, 2007.

[15] P. F. Hokayem and M. W. Spong, "Bilateral teleoperation: An historical survey," *Automatica*, vol 42, no 12, pp. 2035-2057, Dec. 2006.

[16] M. Tavakoli, A. Aziminejad, R. V. Patel and M. Moallem, "High-Fidelity Bilateral Teleoperation Systems and the Effect of Multimodal Haptics," *IEEE Trans. Syst. Man Cybern.*-Part B, vol. 37, no. 6, pp. 1512-1528, Dec. 2007.

[17] R. A. Horn and C. R. Johnson. Matrix Analysis. *Cambridge University Press*, 2013.

[18] The Rover Team, "Characterization of the Martian Surface Deposits by the Mars Pathfinder Rover, Sojourner," *Science*, vol. 278, no. 5344, pp. 1765-1768, Dec. 1997.

[19] W. Li, L. Ding, H. Gao, Z. Deng and N. Li, "ROSTDyn: Rover simulation based on terramechanics and dynamics," *J. Terramech.*, vol. 50, pp. 199-210, 2013.

[20] M.C. Cavusoglu, D. Feygin and F. Tendick, "A Critical Study of the Mechanical and Electrical Properties of the PHANToM Haptic Interface and Improvements for High Performance Control," *Presence: Teleoperators & Virtual Environments*, vol. 11, no. 6, pp. 555-568, Oct. 2002.

[21] W. Li, Z. Liu, H. Gao, L. Ding, N. Li and Z. Deng, "Soil Parameter Modification Used for Boosting Predictive Fidelity of Planetary Rover's Slippage," *J. Terramech.*, vol. 56, pp. 173-184, 2014.

Weihua Li received his BSc and MSc degrees in Manufacturing Engineering of Aerospace Vehicle in Harbin Institute of Technology in 2009 and 2011. He is now working toward his PhD degree in Manufacturing Engineering of Aerospace Vehicle in Harbin Institute of Technology. His research interests include the dynamics, simulation and teleoperation of wheeled mobile robots.

Liang Ding (M' 10) received the PhD degree in Mechanical Engineering from the Harbin Institute of Technology in 2010. He is currently a Professor with the School of Mechatronics in Harbin Institute of Technology.
His research interests include mechanics (terramechanics), control and simulation for robots and mechatronic systems, particularly for planetary exploration rovers and legged robots.

Zhen Liu is an assistant professor in the School of Mechatronics Engineering, Harbin Institute of Technology, China. He received his BSc and MSc degrees in Mechanical Engineering in Harbin Institute of Technology in 2006 and 2008. He received his PhD degree in Mechanical Design in Harbin Institute of Technology in 2013. His research interests focus on the areas of mobile robotics and systems control.

Weidong Wang works with State Key Laboratory of Robotics and System, Harbin Institute of Technology. He received the BSc, MSc and PhD degrees in Mechatronics Engineering from Harbin Institute of Technology in 2002, 2004 and 2009, respectively. His research expertise is in the general areas of robotics and mechatronics. His research interests include motion planning, computer vision and human–machine interaction, and its application in field robot and surgery robot.

Haibo Gao received the MSc and PhD degree in Mechanical Engineering from Harbin Institute of Technology, China, in 1995 and 2003, respectively. He is now a Professor and Vice Dean in School of Mechatronics, and the Vice Dean of State Key Laboratory of Robotics and System in Harbin Institute of Technology.
His research interests mainly focus on mobile robots, aerospace mechanism and control and multi legged robots.

Mahdi Tavakoli (M' 08) is an Associate Professor in the Department of Electrical and Computer Engineering, University of Alberta, Canada. He received his BSc and MSc degrees in Electrical Engineering from Ferdowsi University and K.N. Toosi University, Iran, in 1996 and 1999, respectively. He received his PhD degree in Electrical and Computer Engineering from the University of Western Ontario, Canada, in 2005. In 2006, he was a post-doctoral researcher at Canadian Surgical Technologies and Advanced Robotics (CSTAR), Canada. In 2007-2008, he was an NSERC Post-Doctoral Fellow at Harvard University, USA. Dr. Tavakoli's research interests broadly involve the areas of robotics and systems control. Specifically, his research focuses on haptics and teleoperation control, medical robotics, and image-guided surgery. Dr. Tavakoli is the lead author of Haptics for Teleoperated Surgical Robotic Systems (World Scientific, 2008).